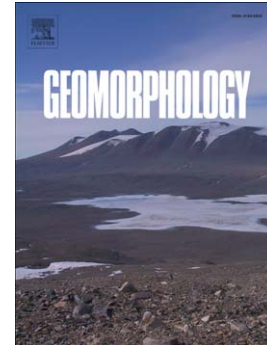# Accepted Manuscript

Morphotectonic and neotectonic control on river pattern in the Sierra de la Cantera piedmont, central Precordillera, province of San Juan, Argentina

Laura P. Perucca, Martín Rothis, Horacio N. Vargas

Please cite this article as: Perucca, Laura P., Rothis, Martín, Vargas, Horacio N., Morphotectonic and neotectonic control on river pattern in the Sierra de la Cantera piedmont, central Precordillera, province of San Juan, Argentina, *Geomorphology* (2013), doi: 10.1016/j.geomorph.2013.09.014

Morphotectonic and neotectonic control on river pattern in the Sierra de la Cantera piedmont, central Precordillera, province of San Juan, Argentina

Laura P. Perucca[1,2] , Martín Rothis[2,3] and Horacio N. Vargas[4]

[1] *Departamento Geología. FCEFyN-UNSJ. Av. Ignacio de La Roza y Meglioli 5400–San Juan.*

[2] *CONICET, Gabinete de Neotectónica. INGEO-FCEFyN-UNSJ. Av. Ignacio de La Roza y Meglioli 5400-San Juan. E-mail: lperucca@unsj-cuim.edu.ar*

[3]*INPRES, Instituto Nacional de Prevención Sísmica*

[4]*CHISÑANCO SRL*

Abstract

The drainage pattern on the western piedmont of the Sierra de La Cantera is divergent, typical of alluvial fans and showing anomalies that are directly related to the trace of La Cantera thrust. In previous studies, two types of anomalies were identified: upstream of the fault scarp, rivers have a broom-shaped pattern, while downstream -in the hanging block- streams become denser, more sinuous and incised. In this contribution, these morphotectonic aspects were analyzed in detail, making direct and indirect analysis to quantify the relationship between these anomalies and the faults affecting alluvial fans. In addition, the influence of neotectonic activity on smaller water course patterns in the alluvial fan areas was investigated in order to find indicators of on-going vertical movements, since the spatial arrangements of these piedmont channels are determined by slope and structure, where active faults cause diversions or anomalies. Topographic profiles in two selected channels cutting across the trace of the fault were performed using a differential GPS in order to establish the relationship between the sinuosity and slope of these rivers. The results obtained allow us to state that the most sinuous channels have lower slopes and are located in the hanging wall of the fault. Morphometric analysis of scarps stated that active tectonics have played an essential

role in controlling the drainage pattern in the piedmont, leading the rivers to adjust to these slope variations.

Finally, based on the geomorphologic, stratigraphic, structural and seismological characteristics and parameters analyzed, La Cantera Thrust is considered a seismogenic source of significance to the nearby towns (>700,000 inhabitants) and also to the large-scale dams built downstream along the San Juan River.

Keywords: Neotectonics, La Cantera thrust, river pattern anomalies, Precordillera, Argentina

Introduction

Rivers react quickly and consistently to active tectonic deformation of the Earth's surface reflecting subtle changes in topography (Seeber and Gornitz, 1983; Ouchi, 1985; Holbrook and Schumm, 1999; Jain and Sinha, 2005; Turowski et al., 2006; Amos and Burbank, 2007). When alluvial rivers develop under tectonic deformation, some pattern responses such as the morphology of the channels and the equilibrium profile are observed. Rivers respond and adjust to deformation, thus a variation of river morphology or channel behavior can be anticipated (Ouchi, 1985; Schumm et al., 2002). So, the analysis of the drainage pattern is an important tool in the study of tectonic activity in thrust fault systems since they are highly sensitive to vertical tectonic uplifts related to folds and thrusts (Audemard, 1999). Some features that could be identified from these kind of studies are river diversion, beheaded streams, captured streams, changes in the incision depth, sinuosity and river gradient along stream, and other geomorphologic characteristics such as wind gaps, sag ponds, tectonic gutters and broom-shaped river patterns reflect changes induced by active tectonics.

La Cantera thrust, located in the western piedmont of Sierra de La Cantera, extends along more than 40 km in the Central Precordillera. This Quaternary fault exhibits considerable evidence of drainage anomalies that has been studied by Millán and

Perucca (2011). However, no previous works have referred to these issues in other regions of the Central Andes of southern South America, and geomorphic indicators have not yet been used as tools to characterize sectors deformed by active pure dip-slip thrust faults with low to moderate deformation rates, in fold and thrust belts associated with thin-skinned. Thus, the aim of this work is to quantify the deformation observed in the drainage pattern of La Cantera piedmont through a detailed study of the changes in the river gradient, sinuosity index, river incision, and the relation of the morphotectonics with these parameters. From this study we will be able to explain the high variability of small streams affected by Quaternary faults, the resulting anomalous drainage patterns, and their relevance as indicators of the nature and location of areas with observed or likely active tectonics. Also, the results obtained will allow a better understanding of the neotectonic evolution of this key part of the Andean thrust.

Study area

The analyzed area is located in a tectonic valley between Sierra de La Cantera and La Invernada in the Central Precordillera geological province (Fig. 1a,b), located at the center of the Province of San Juan (31º 04' - 31° 10'S and 69º 01' - 68° 58'W) in the department of Ullum, northwest of San Juan city, Argentina. The Sierra de La Invernada stands out as a mountain chain elongated from north to south, with a maximum height of 3,700 m asl. The Sierra de La Cantera also has north-south trend and a height of 3,100 m asl. Main streams, which are located in the eastern foothills of the Sierra de La Invernada and western piedmont of Sierra de La Cantera, drain from Mogote La Leona hills northward to the Pampa de Gualilán basin, the local base level. Pampa de Gualilán is an endorheic basin, which receives the contribution of the most important drainage network of the region (Fig. 1a,b).

Among previous research in the area we draw attention to Whitney and Bastías (1984) who briefly described features with Quaternary tectonic activity in the western piedmont of the Sierra de La Cantera, north of the San Juan River. Also Mingorance (1998), who recognized two sections of interest along the fault: the

northern section that is characterized by increased Quaternary tectonic activity in the mountain fronts and higher shallow historical seismicity; and, the southern sector where Quaternary deformation is concentrated almost exclusively in the intermountain valley, with faults affecting the piedmont and the limited tectonic activity in the mountain fronts. Based on the analysis and quantification of paleoseismic indicators, Mingorance (1998) also identified that at least three individual seismotectonic events of varying magnitude and located along the La Cantera fault were generated by the fault in prehistoric and historic times. The last historic event occurring in the northern sector was the 1924 earthquake (Ms = 6.0). Millán and Perucca (2011), carried out the analysis of five natural trenches located in the northern section of the fault and briefly mentioned some drainage anomalies in the area. However, these authors discuss the presence of many anomalies that take place where rivers cross the La Cantera fault trace, like the apparent increase in the degree of incision and sinuosity of the network channels and the change from a divergent pattern (typical of alluvial fans) to a broom-shaped drainage. This broom-shaped drainage includes a series of water courses of a basin which are grouped to increase their flow in order to cross an active structure that is opposed to the natural flow. This is an array of diverted, adapted and deflected drainages by regressive erosion, capture or obstruction. Audemard (1999) recognized these anomalies in the drainage pattern of active thrusts in Venezuela and Colombia, highlighting their importance as indicators of vertical motion produced by these thrusts.

In the study area, from north to south, broom-shaped drainage anomalies, river diversion captures and wind gaps developed on Quaternary piedmont deposits are indicative of the La Cantera fault trace (Figs. 1a, 2). It is possible to recognize a higher density of these anomalies in the northern trace, possibly related to tectonic reactivation in recent times.

The change in depth of the incision channel, gradient and meander pattern along the drainage streams are also indicators of vertical movement. Even the smallest changes in the topography affect the sinuosity of low gradient rivers (Holbrook and Schumm, 1999), implying on-going microtopographic changes. Under certain conditions, alluvial rivers tend to evolve as single meandering channels (Zámolyi et

al., 2010). The meandering pattern changes as vertical tectonic movements influence the piedmont slope. Besides, it is possible to see that rivers follow meandering courses and exhibit a highly sinuous and incised channel where drainage pattern becomes denser when they cross the hanging block of La Cantera thrust. This drainage density increases with the percentage of silt-clay content of Neogene rocks outcropping in the hanging block (Fig. 2).

Tectonic setting

Between 29º and 33º latitude south and with a convergence azimuth of around 78º (Vigny et al., 2009), the Nazca plate is being subducted at a rate of 6.3 cm/year beneath the South American plate to depths of up to 100 km (Ramos, 1988, 1999; Kay et al*.,* 1991; Kay and Mpodozis, 2002; Kendrick et al., 2003). The flat geometry of the subducted slab is attributed to the oblique subduction of the Juan Fernández ridge beneath the South American plate (Pilger, 1981; Anderson et al., 2007; Alvarado et al., 2009; Martinod et al., 2010; Rosenbaum and Mo, 2011) (Fig. 1c). In this area, Late Miocene-Quaternary tectonics has resulted in the development of the Principal and Frontal Cordilleras, Precordillera and the Sierras Pampeanas in the eastward foreland region (Ramos, 1988, 1999; Ramos et al., 2002). Beck et al. (2008) and Alvarado et al*.* (2009) refined the location of earthquakes in the flat-slab near 30°-31°S and showed that the shallowest portion of the slab is associated with the subducting Juan Fernandez ridge.

The Central Precordillera is formed by mountain ranges extending from latitudes 29º to 32ºS. It has been described by several authors (Jordan et al*.,* 1983, 1993; Allmendinger et al*.,* 1990; von Gosen, 1992; Cristallini and Ramos, 2000) as a characteristic thin-skinned, thrust-and-fold belt due to Neogene crustal shortening on west dipping, imbricated structures that root down to a 10-15 km-deep main décollement. In this region, most of the active structures are related to compressional faulting. However, earthquakes on these active reverse faults are not always accompanied by surface ruptures.

A series of geologic and tectonic factors occurs where the Nazca plate is subducted sub-horizontally, between 29º and 33º latitude south,which seem to be related to surface seismic activity, and a substantial part of the Quaternary deformations in Argentina are concentrated in this region (Costa et al., 2006). Here the main seismogenic sources can be located and defined with certitude although these sources show different degrees of activity. Generally, they are sub-parallel faults, predominantly N-S trending, which are located in the intraplate setting where the most important destructive earthquakes took place. The latter were related to surface ruptures, such as the earthquakes of 1894 (Ms = 7.5), 1944 (Ms= 7.4), and 1977 (Ms = 7.4), and also all of them occurred between these latitudes (Perucca et al., 2006).

The geology of the area is characterized by fine and coarse sandstones to fine conglomerates of Pachaco Formation of Eocene to Late Miocene age (Milana et al., 1993) that outcrop in the western piedmont of Sierra de La Cantera, commonly associated with fault zones. The sandstones have a westward-dipping homoclinal structure produced by reverse faulting of the west-dipping La Cantera active fault. Neogene rocks are covered by Quaternary alluvial deposits. On the surface, this fault zone primarily affects Neogene and Quaternary stratigraphic units.

Data and Methods

Fault detection can be improved by interdisciplinary methods such as satellite images and aerial photography analysis, field control, and trench revision. Uplifting zones considerably affect the river courses of a piedmont since they react as sensors, modifying their courses according to the meso and micro-topographic changes due to the differential uplift-subsidence patterns, so that under certain conditions low sinuosity rivers tend to evolve as a meandering system, increasing their sinuosity. In this study, we analyzed the changes in sinuosity in the vicinity of faults as this behavior is influenced by tectonic movements which are reflected in the parameters of fluvial channels. Many researchers have documented the influence of vertical movements on the channel pattern, such as Ouchi (1985), Keller and Pinter (1996), Holbrook and Schumm (1999) and Zámoly et al. (2010), among others.

In this research, a detailed fault scarp data have been acquired with a differential GPS by measuring high-resolution topographic profiles perpendicular to the fault scarps and along two incised gullies (Figs.3-5). In order to highlight the topography of the terrain in detailed high resolution elevation sections, the profiles were selected considering easy-access to the sections to improve the coverage with the measurement devices. A detailed photo-interpretation of the area allowed the final selection of two NW transects perpendicular to the fault scarps, two longitudinal profiles along two rivers to highlight particular morphological patterns and transects in random directions to increase the population of data and improve the resolution of the modelling. Also, classic sinuosity values and slopes were calculated for two streams that cross the fault. The equipment used was a GPS differential system, with a high performance GPS/SBASS L1 receiver, that also has EVEREST signal filtering technology. The measurements were performed with the following routine: the positioning and configuration of each device in manual mode, selecting record every 2-second intervals, mask angle of 10 and track times of 2 seconds. For collection of the field data,one of the devices was stationed at one point and the other was used as a rover. The processing of field data included correction of data using software provided by the differential GPS system. With these data, the digital elevation models (DEMs) were generated, using different interpolation methods (such as triangulation, least squares, kriging, among others). The DEM selected was created with the triangulation method because it was the best one that represents the real topography. The data from the high resolution elevation profiles perpendicular to the fault scarp (section A-A' and B-B' figure 5) and those from the longitudinal profiles were also applied to create high-resolution topographic profiles and to determine the slope changes in each transect. Additional inspection for the presence of scarps was completed through the study of a 100 m grid-spaced digital elevation model (DEM) accented by hill-shaded relief.

The two profiles were carried out along two temporary channels transverse to the fault zone. Each profile (north and south) was sub-divided into a number of sections according to the presence of Quaternary fault evidence present in each section of its slope and channel sinuosity index (Figs. 3, 4). The sinuosity of streams from the

Sierra de La Cantera in the vicinity of faults were also analyzed together with other morphostructural elements recognized in the piedmont were analyzed.

The southern river was analyzed only in a section, since downstream of the fault zone human activity has modified and masked the stream. A quantitative measure of the variation of the meandering pattern is the sinuosity index. The sinuosity index (S) of a stream is obtained from the relationship between the length of the channel (C) and the valley length (V) (Keller and Pinter, 1996) (1).

$$S = C/V \qquad (1)$$

The S values were calculated using the digitalized planforms of the stream water courses using a GIS. Several window sizes were used, depending on the segments formed by the parallel thrusts.

On each of the segments slope values were also estimated, and the shape of the path of the channel in a plan view according slope changes was also observed. For each one, the spatial relationship between the slope and the sinuosity of the channels was observed, allowing the determination of drainage parameters.

To the North Channel, the profile obtained is 1.5 km in length and an elevation of 70 m, trending NNW. In the satellite image and plan view (Fig. 3a) the location of the counter-slope escarpments and their relationship with the drainage can be observed. Moreover, the South channel profile (Fig. 4a) is 1.0 km in length and 65 m in elevation. In both channels the increase observed in the degree of sinuosity and incision is coincident with the main trace of the La Cantera thrust (Figs. 3c,d;4c,d).

Results achieved in the analyzed channels indicate the close relationship between the sinuosity of a channel with its longitudinal profile slope, consistent with those obtained by Silva et al. (1988) and Jain and Sinha (2005), among others (Figs. 3a,b; 4a,b). Thus, in most of the surveyed channels, the sinuosity becomes larger when the river profile slope is smaller, and vice versa, unlike the results obtained in experiments (Ouchi, 1985).

The two detailed topographic profiles (A-A' and B-B') trending E-W, were performed perpendicular to the main east-facing fault and several parallel scarps. In

determining the placement of the two transects across the escarpments, the following considerations were taken, such as to define an equidistance between profiles that ensures including the largest area of the selected section, and avoiding the presence of any modification of the relief that is non-tectonic in nature, like those produced by natural erosion of channels parallel to the base of the escarpments, gullies, rills, etc

The equidistance between surveyed points in each transect was 50 cm and between transects of about 200 m. This analysis allowed the authors to define five sub-parallel scarps that were referred, from east to west, as scarp 1, 2, 3, 4 and 5 (Fig. 5c), that is so because thrusting characteristically distributes slip on multiple imbricate faults (Mc Calpin, 2009). Furthermore, the geomorphological features analyzed in this work together with the trenches analyzed and dated by Millán and Perucca (2011) indicate Holocene tectonic activity to escarpment 1, affecting along its trace mid-Holocene soil horizons and Holocene alluvial terraces.

In addition, a DEM of the area between the two river profiles, which shows the shape of the ground with clear evidence of Quaternary tectonic activity, was prepared (Fig. 5a,b), since high-resolution digital elevation models (DEMs) have recently been used as an important tool for highlighting fault scarps (Delvaux et al., 2007; Songmuang et al., 2007; Frankel et al., 2010).

Maximum magnitude earthquake was estimated by using the empirical relationships developed by Wells and Coppersmith (1994) for rupture length. The average slip rate and recurrence were estimated with the offset of a middle Holocene soil and one historical earthquake with its epicenter in the north of the area.

Results and discussion

La Cantera thrust is a 47 km long, N-S trending structure that runs on the western piedmont of the Sierra de La Cantera. The fault affects Quaternary alluvial deposits that overlie unconformably the Neogene strata and form continuous and well-preserved counter-slope east-facing scarps (Fig. 6a). Along the whole segment of the mapped La Cantera thrust, the fault consists of one well-defined trace, marked

by features described below, and several traces that are parallel or sub-parallel to the main trace.

The east-vergent faults trend 200º and dip 10º to 30º W, with simple and compound counter-slope scarps (Figs. 6a,b,c). The height of scarps in the northern section varies between 0.3-6.0 m. La Cantera thrust affects all alluvial levels of the piedmont and modifies the existing drainage pattern. The piedmont is still active, as suggested by both a well-developed network of braided and sinuous streambeds incised ~1.0 m into it, and a well-preserved surface morphology with bars and swales formed by slightly varnished sub-angular cobbles.

The main thrust surface separates Neogene rocks (Ne) from Quaternary alluvial deposits (Q) (Fig. 6b,c). The ^{14}C dating of a soil level affected by the fault yields a radiocarbon age of 4,580 ± 50 years BP with an estimated ^{12}C/^{13}C ratio of -5‰ ± 2 (Millán and Perucca, 2011). Pure vertical displacement is deduced from the morphology of the slickenside, with a pitch of 90º.

Along the La Cantera fault area, the best exposed geomorphic evidence and most recurrent expressions of tectonic activity are anomalies of drainage patterns, flexural scarps, multiple antislope scarps (Fig. 6d), sag ponds (Fig. 7a), three stair cased alluvial terraces entirely located in the hanging block and progressive deformation with increasing time (Figs. 2, 6, 7b), and aligned springs (Fig. 7c). This geomorphic evidence suggests current tectonic activity of the La Cantera thrusts.

Flexural scarps are recognized at the front of the active thrust with a warping of the fanglomerate deposits at the shallow tip of the blind thrust (Fig. 2). Moreover, the alignment of springs is another indicator of the fault trace, together with the presence of sag ponds on the streams because of the counter-slope scarps, implying that erosion by river flow is subordinate to tectonic uplift. In addition, wind gaps and beheaded streams were observed in the hanging block of the fault and revealed that no river is draining it at present (Fig. 2).

Small rivers that drain the western piedmont of the Sierra de La Cantera often reflect subtle topographic modifications. River diversion is one of the most conspicuous features recognized along the fault trace, suggesting that the tectonic uplift rates are faster than the linear stream erosion rates (Fig. 2).

The river beds are also sensitive to variations in the longitudinal slope of the channel (Schumm, 1986; Schumm et al., 2002). The latter may be due to lithological contrasts or as a result of tectonic activity. Ouchi (1985) pointed out that when active tectonics prevails, channel gradients change. So, alluvial rivers respond to active tectonic movement in ways that depend on the nature of deformation and the characteristics of the river. Upstream of La Cantera thrust, channels are straight and wide, but when crossing the fault, they become narrow and sinuous (Figs. 2-4). Another characteristic feature is the change of incision depth along river courses (Figs. 4-7d,e). Incision rate can increase with decreasing slope. Also the drainage pattern becomes denser and more sinuous where streams cross the hanging block of the La Cantera thrust (Figs. 2, 7b). The analysis of longitudinal profiles along two rivers by using differential GPS, revealed the presence of vertical motion, with incision increasing and the change of the river pattern from straight to meandering, in order to try to maintain a constant gradient (Figs. 4-7b,d,e). It is possible to observe that, in Fig. 3c, the channel slope decreases in the first section, when passing through scarps 1 and 2 (Fig. 4a), and then remain constant. Fig. 4c shows an abrupt change in slope when the stream crosses the first fault, and then remains more or less constant. In the tables it is also possible to observe the increase in the sinuosity of channels at the same time that the longitudinal slope values decrease (Figs. 3d,4d).

Most of the rivers coming from the Sierra de La Cantera gather to cross the fault, showing a broom-shaped pattern to overcome the vertical growth of the E-facing scarp, which is a characteristic feature along the entire fault trace (Fig. 2). Finally, the morphotectonic features observed include progressive unconformities (Fig. 7f), close to the flexure and three staircased alluvial terraces exclusively presented in the hanging wall block, the younger a fill terrace and the older, strath terraces (Fig. 7b). Here, the La Cantera thrust trends perpendicular to the streams and incision has occurred in response to recent uplift. The terraces successively increase in height above the actual channel; the youngest terrace is ~1.0 m above the modern-day channel, the intermediate terrace is ~2.0 m above the channel, and the oldest one is ~3.5 m above the channel bottom. The youngest terrace is a fill terrace whilst the

two older ones are strath terraces. The presence of these terraces are related to the uplift of the hanging wall which produced the progressive incision of the streams, similar to the formation of the strath terraces in the Höh Serh–Tsagaan Salaa fault system in the Mongolian Altai in central Asia, although in this case, terraces were triggered by the migration of the knickpoint formed instantaneously during ground-rupturing earthquakes (Frankel et al., 2010).

Similarly, near the La Cantera fault, the three abandoned terraces should correlate with repeated co-seismic events, although no detailed geomorphic and chronologic studies have been performed yet.

Shaded relief renditions of the resulting ground DEM revealed geomorphic features associated with five counter-slope fault scarps (Fig. 5 a,b). Indeed, the DEM has resulted in the identification of four previously unrecognized linear topographic scarps parallel to the main fault, briefly described in previous research (Whitney and Bastías, 1984; Millán and Perucca, 2011), all of which relate to Quaternary surface-rupturing earthquakes. Two topographic profiles extracted from the DEM across the east-facing fault scarps were analyzed (Fig. 5a,c). The height of the five scarps ranges from 0.20 cm (scarp 2) to 8 m (scarp 4). We interpret active imbricated thrusts verging to the east with a low angle, <500 m-wide, with five rounded scarps that trend roughly parallel. This shape may be influenced by the properties of displaced materials (Stewart and Hancock, 1990). Where the surface material is weak (poorly consolidated Quaternary sediments and Neogene sandstones/siltstones), internal warping resulted in the formation of a topographic flexure. A relatively young fault scarp can also be modified by erosion (Stewart and Hancock, 1990). However, further studies are required to confirm this hypothesis.

A trenching study at the northern part of the La Cantera thrust made by Millán and Perucca (2011) revealed at least two events caused by paleo-earthquakes, with the most recent expressed as a reverse fault off-setting a poorly-developed soil (4,580 ± 50 radiocarbon years BP) with a historical event with Ms = 6.0.

By using various empirical relationships for the fault displacement and the surface-length rupture like the ones derived from Wells and Coppersmith (1994), we estimate moderate to large paleo-earthquakes (M 6 – 7.1) for this fault, which is in

agreement with the tectonic context of an intraplate zone of the Precordillera region. Moreover, we have obtained the recurrence interval for these paleo-earthquakes of 2.5 kyr ($6 < M < 7$) and a fault slip of 0.1 to 0.5 mm/yr by plotting these values along the Slemmons (1982) curve (moderate activity with moderate to well-developed geomorphic evidence of activity).

Conclusions

La Cantera thrust, located in the intermontane valley between Sierra de La Cantera and Sierra de La Invernada, has provided remarkable geomorphological evidence of Quaternary tectonic activity. We identified at least five east-facing faults scarps in the northern portion of La Cantera Thrust. All of them show geomorphic evidence for recent activity, such as well-preserved escarpments, drainage anomalies, stair-paired terraces, sag-ponds and aligned springs. Meso-scale structures recognized in the Quaternary sediments confirm that Pliocene-Pleistocene deformation has continued into the Holocene, highlighting the late Quaternary activity of the La Cantera thrust.

Analysis of the drainage network anomalies allowed definition of the trace of the La Cantera thrust. A divergent pattern was defined for the study area, typical of alluvial fans but, due to the strong influence of the hanging block of the fault when the rivers cross, it undergoes some changes in the drainage pattern. We also determined that in the hanging block, streams are incised and denser. In addition, all alluvial levels are affected by the trace of the faults.

Comparison of the distribution of the sinuosity along channels in the sector analyzed, under certain lithological and geomorphological features, reveals that changes in the values of sinuosity reflect neotectonic activity.

The study of the longitudinal profiles of these channels that cross the piedmont show a significant departure of the profile of these streams with respect to the theoretical equilibrium profile, all of which are affected by inflections, the positions of which are determined by the trace of the fault perpendicular to them.

Sinuosity variations along confined streams in the Neogene section are related to a differential uplift of thrusts which are closely related to slope changes in the longitudinal slope profile of each channel, where low slopes are related to high sinuosity meandering channels. Thus, reverse faults verging in the up-drainage direction causes increasing meandering.

Therefore, active tectonics have also played an important role in controlling the drainage pattern in the western piedmont of the Sierra de La Cantera, causing the tributaries to adjust to even the most subtle slope changes of the piedmont. Comparison of the sinuosity distribution along the tributaries with geomorphological and structural features reveals these changes.

Usage of DEMs and the study of drainage patterns is a useful tool that evidences vertical uplifts but no horizontal displacements. We were able to confirm that all the fault segments and scarps analyzed from the fieldwork and DEM were identified as active faults, based on the similarity of the geomorphic and kinematic data.

Deterministic formulas that take into account the complete length of La Cantera thrust resulted in earthquakes of magnitudes 6.0 to 7.1, with a recurrence time of 2.5 ka years. For these reasons and the profuse geomorphologic evidence of active tectonics described and discussed in this contribution, the seismogenic potential for this fault, located near the town of San Juan (>700,000 inhabitants) and of three dams located downstream along the San Juan River, should not be underestimated.

References

Allmendinger R., Figueroa, D., Zinder, E., Beer, J., Mpodozis, C., Isacks, B. L., 1990. Foreland shortening and crustal balancing in the Andes at 30º latitude. Tectonics 9, 789-809.

Alvarado, P., Pardo, M., Gilbert, H., Miranda, S., Anderson, M., Saez, M., Beck, S.L., 2009. Flat–slab subduction and crustal models for the seismically active Sierras Pampeanas region of Argentina, *in* Kay, S., Ramos, V.A., Dickinson, W. (eds.), MWR204: Backbone of the Americas: Shallow subduction, plateau uplift, and ridge and terrane collision: Boulder, Colorado, Geological Society of America, 261–278.

Amos, C. B., Burbank, D. W., 2007. Width of channel belt response to differential uplift. Journal of Geophysical Research, 112, F0201.

Anderson, M., Alvarado, P., Zandt, G., Beck, S.L., 2007.Geometry and brittle deformation of the subducting Nazca Plate, central Chile and Argentina. Geophysical Journal International 171(1), 419–434.

Audemard, F., 1999. Morpho-structural expression of active thrust fault systems in the Humid Tropical Foothills of Colombia and Venezuela. Zeitschrift fur Geomorphologie 118, 1-18.

Beck, S., Alvarado, P., Wagner, L., Anderson, M., Gilbert, H., Zandt, G., 2008. Flat-slab subduction beneath the Sierras Pampeanas in Argentina. 7th International Symposium on Andean Geodynamics Extended Abstracts, 75-76. Nice.

Costa, C., Audemard, F., Bezerra, H., Lavenu, A., Machette, M., Paris, G., 2006. An overview of the main Quaternary deformation of South America. Revista de la Asociación Geológica Argentina 61 (4), 461-479.

Cristallini, E.O., Ramos, V.A., 2000. Thick-skinned and thin-skinned thrusting in the La Ramada fold and thrust belt: crustal evolution of the High Andes of San Juan, Argentina (32° SL). Tectonophysics 317, 205-235.

Delvaux, D., Macheyeki A.S., Kervyn, F., Petermans T.; Verbeeck, K., Temu, E.B., 2007. Earthquake geology of the Kanda fault system (Tanganyika-

Rukwa rift, SW highlands of Tanzania). Geophysical Research Abstracts 9, 09129

Frankel, K. L.,Wegmann, K. W., Bayasgalan, A, Carson, R. J.,Bader, N. E., Adiya, T., Bolor, E.,Durfey, C. C., Otgonkhuu, J.; Sprajcar, J.; Sweeney, K. E.;Walker, R. T.,Marstellar, T. L., Gregory, L., 2010. Late Pleistocene slip rate of the Höh Serh–Tsagaan Salaa fault system, Mongolian Altai and intracontinental deformation in central Asia. Geophysical Journal International 183 (3), 1134-1150

Holbrook, J., Schumm, S.A., 1999. Geomorphic and sedimentary response of rivers to tectonic deformation: a brief review and critique of a tool for recognizing subtle epirogenic deformation in modern and ancient settings. Tectonophysics 305, 287-306.

Jain, V., Sinha, R., 2005. Response of active tectonics on the alluvial Baghmati River, Himalayan foreland basin, eastern India.Geomorphology70, 339-356.

Jordan T.E., Allmendinger R.W., Damati J.F., Drake R.E., 1993. Chronology of motion in a complete thrust belt: the Precordillera, 30-31ºS, Andes Mountains. Journal of Geology 101, 137-158.

Jordan, T.E, Isacks, B., Allmendinger, R.W., Brewer, J., Ramos, V., Ando, C., 1983. Andean tectonics related to geometry of subducted Nazca plate. Geological Society of America Bulletin 94, 341-361.

Kay, S.M., Mpodozis, C., 2002. Magmatism as a probe to the Neogene shallowing of the Nazca plate beneath the modern Chilean flat slab. Journal of South American Earth Sciences 15, 39-59.

Kay, S., Mpodozis, C., Ramos, V., Munizaga, F., 1991.Magma source variations for mid-late Tertiary magmatic rocks associated with a shallowing subduction zone and a thickening crust in the central Andes (28º to 33º S). In Harmon, R. S. y Rapela, C.W. (eds.) Andean Magmatism and its Tectonic Setting, Geological Society of America, Special Paper 265, 113-137.

Keller, E.A., Pinter, N., 1996. Active tectonics: earthquakes, uplift, and landscape. Prentice Hall eds. Upper Saddle River, 337 p., New Jersey.

Kendrick, E., Bevis, M., Smalley, R.J., Brooks, B., Vargas, R.B., Lauría, E., Fortes, L.P., 2003. The Nazca-South America Euler Vector and its Rate of Change.Journal of South American Earth Sciences 16, 125-131.

Martinod, J., Husson L., Roperch, P., Guillaume, B., Espurt, N., 2010. Horizontal subduction zones, convergence velocity and the building of the Andes. Earth and PlanetaryScienceLetters 299, 299–309.

Mingorance, F., 1998. Evidencias de paleoterremotos en la falla activa La Cantera-Cinturón de empuje de la Precordillera, San Juan, Argentina: 10° Congreso Latinoamericano de Geología Actas 2, 161-166.

Milana, J. P., Cevallos, M., Zavattieri, A., Prampano, M., Papu, H., 1993. La secuencia terciaria de Pachaco: sedimentológica, edad, correlaciones y significado paleogeográfico. 12° Congreso Geológico Argentino y 2° Congreso de Exploración de Hidrocarburos 1: 226-234.

Millán, J.L., Perucca, L.P., 2011. Análisis neotectónico del extremo norte del sobrecorrimiento La Cantera, provincia de San Juan, Argentina. Revista Mexicana de Ciencias Geológicas 18(3), 337-348.

Ouchi, S., 1985. Response of alluvial rivers to slow active tectonic movement.Geological Society of America Bulletin 96, 504-515.

Perucca, L, Pérez, M., Navarro, C., 2006. Fenómenos de licuefacción asociados a terremotos históricos. Su análisis en la evaluación del peligro sísmico en la Argentina. Revista de la Asociación Geológica Argentina 61 (4), 567-578. Buenos Aires.

Pilger, R.H., 1981. Plate reconstructions, aseismic ridges, and low angle subduction beneath the Andes. Geological Society of America Bulletin 92, 448-456

Ramos, V., 1988. The tectonics of the Central Andes; 30º to 33ºS latitude, In: Processes in Continental Lithospheric Deformation. S. Clark and C. Burchfiel (Eds.). Geological Society of America, Special paper 218, 31-54.

Ramos, V. A., 1999. Plate tectonic setting of the Andean Cordillera. Episodes 22, 183-190.

Ramos, V.A., Cristallini, E.O., Pérez, D., 2002. The Pampean flat-slab of the Central Andes. Journal of South American Earth Sciences 15, 59-78.

Rosenbaum, G., Mo, W., 2011. Tectonic and magmatic responses to the subduction of high bathymetric relief. Gondwana Research 19, 571-582

Schumm, S. A., 1986. Alluvial river response to active tectonics. In: Active Tectonics. Studies in Geophysics (R. E. Wallace, Ed.). Nat. Acad. Press, Washington 80-94.

Schumm, S. A., Dumont, J. F., Holbrook, J. M., 2002. Active tectonics and alluvial rivers. Cambridge University Press, 292 p. Cambridge.

Seeber, L., Gornitz, V., 1983. River profiles along the Himalayan arc as indicators of active tectonics. Tectonophysics 92, 335-367.

Silva, P., Goy, J., Zazo, C., 1988. Neotectónica del sector centro-meridional de la Cuenca De Madrid. Estudios geológicos 44, 415-427. Spain.

Slemmons, D. B., 1982. Determination of design earthquake magnitudes for microzonation, in Proceedings of the Third International Earthquake Microzonation Conference Vol. 1: Washington, D.C., U.S. National Science Foundation, 119-130.

Songmuang, R., Charusiri, P., Choowong, M., Won-in, K., Takashima, I. and Kosuwan, S. 2007. Detecting Active Faults Using Remote-Sensing Tecnique : A Case Study in the Sri Sawat Area, Western Thailand. Journal of Science Asia, 33, 23-33.

Stewart, S., Hancock, P., 1990. What is a fault scarp? Episodes13, 256-263.

Turowski, J. M., Lague, D., Crave, A., Hovius, N., 2006. Experimental channel response to tectonic uplift. Journal of Geophysical Research 111, F03008.

Vigny, C., Rudloff, A., Ruegg, J.-C., Madariaga, R., Campos, J., Alvarez, M., 2009. Upper plate deformation measured by GPS in the Coquimbo Gap, Chile. PEPI 175, 86–95.

Von Gosen, W., 1992. Structural evolution of the Argentine Precordillera: the Rio San Juan section. Journal of Structural Geology 14 (6), 643-667.

Wells, D.L., and Coppersmith, K.J., 1994. New empirical relationships among magnitude, rupture length, rupture width, and surface displacements: Bulletin of the Seismological Society of America 84, 974-1002.

Whitney, R., Bastías, H., 1984. The Tigre fault of the San Juan Province, Argentina—The late Quaternaryboundary of the Andes uplift: Geological Society of América Program with Abstract16, 6 - 693.

Zámolyi, A., Székely, B., Draganits, E., Timár, G., 2010. Neotectonic control on river sinuosity at the western margin of the Little Hungarian Plain. Geomorphology 122, 231-243.

Figure Captions

Figure 1. a) Location Map of the La Cantera thrust and details of thenorthern end ofthe fault with river profiles location, b) shaded-relief image of 30m-spacing digital elevation model (DEM derived from SRTM data), highlighting the structural and geomorphological array, c) map of central-western Argentina showing upper plate tectonic features (Modified from Ramos et al., 2002).

Figure 2. The oblique Google Earth image shows the geomorphic features which are associated with the active trace of the La Cantera thrust. These features consist of fault scarps, sag-ponds, river diversion, trenches, wind gaps and broom-shaped drainages, among others.

Figure 3.a) View of the North river and related fault scarps; b and c) elevation and slope longitudinal profiles, where it is possible to see changes in both parameters, according to the presence of Quaternary faults. These changes are reflected in the planform of the river. The numbers represent each section of the river analyzed. d) Table summarizing slope and sinuosity values in six sections of the North river, related to fault escarpments.

Figure 4.a) View of the South river and related fault scarps; b) and c) elevation and slope profiles leveled across south river, as in Fig. 3.d) Table summarizing slope and sinuosity values in three sections of South river, related to parallel faults.

Figure 5.a) Google Earth image of the measured area, showing the scarps and selected profiles. b) DEM image of the study area. Differential GPS-derived DEM revealed the five scarps of the La Cantera thrust system. The active thrusts trend N-S and are imbricate, west-dipping reverse thrusts.c) Cross-topographic profiles (A-A' and B-B') displaying the fault scarp heights and shapes. Rounded profiles of fault scarps possible are due to the unconsolidated (alluvium) to weakly consolidated (Neogene) materials easily erodible or by collapse and slope retreat of the scarps.

Figure 6.a) Field photograph of La Cantera thrust showing well-defined simple and compound parallel scarps, b) Natural trench where Neogene (Pachaco Formation) rocks override Late Pleistocene fluvial deposits in the north trace of La Cantera

thrust. The fault trends N-S and dips 10º W. c) Parallel trench to the low‑angle La Cantera thrust, d) view looking to the west. White arrows indicate the five fault scarps measured with the differential GPS and white circles highlight persons for scale.

Figure 7.a) Associated with trenches and the counter slope scarps, there are tectonic depressions filled with fine sediments (sag ponds) and aligned springs (the circle highlights a person for scale). b) Google Earth oblique view showing the adjustment of rivers (black arrows) to the fault scarp changing in some cases from straight to sinuous or/and increasing density of channels. Three unpaired terraces (pointed with white arrows) were recognized only in the northern bank of the streams. c) View to the north with aligned springs with vegetation contrasts. d) Upstream of the fault area, channels are slightly incised and wider. e) Downstream of the main fault, channels are narrow and notably incised. f) Fault-related progressive unconformities in alluvial Pleistocene deposits.
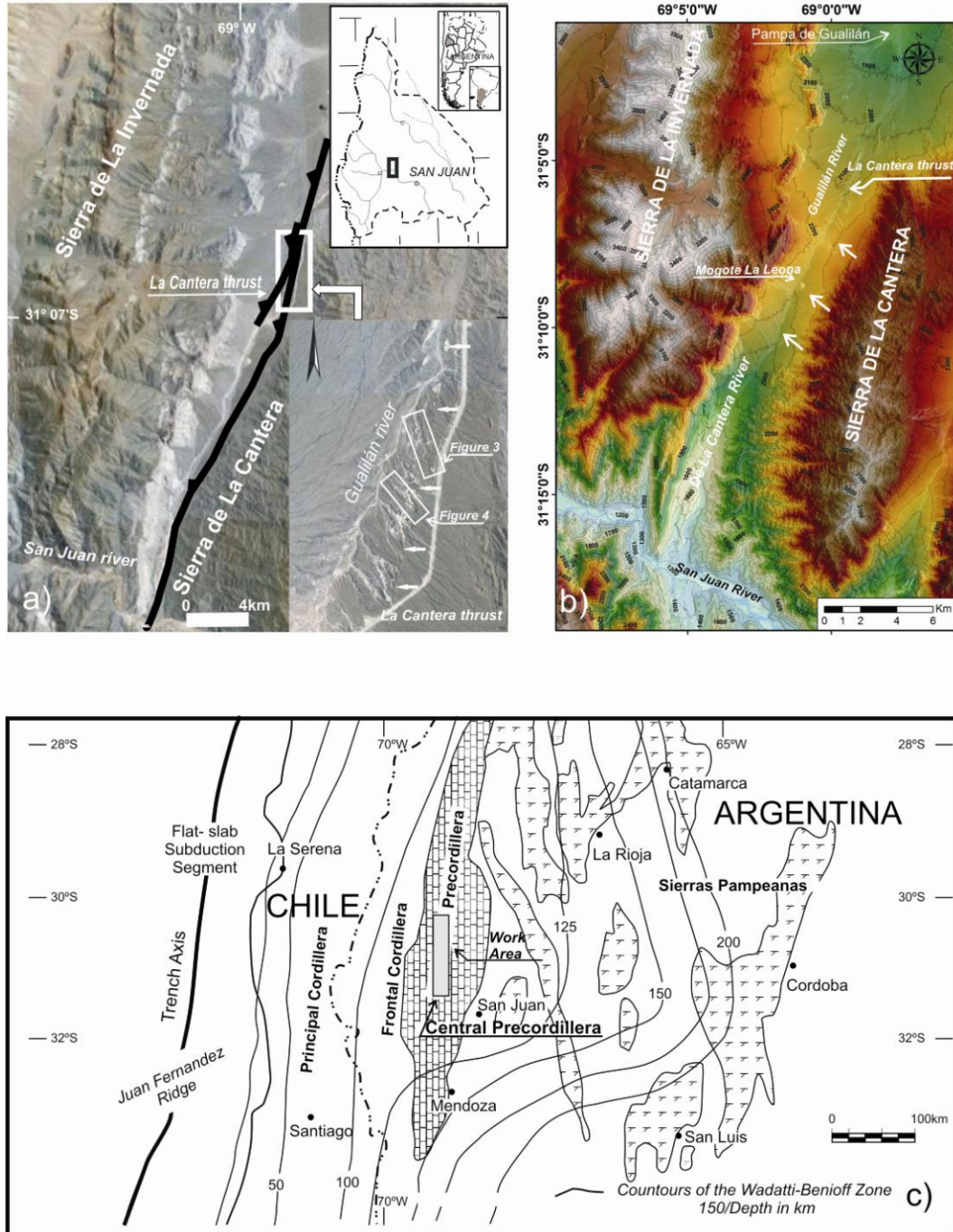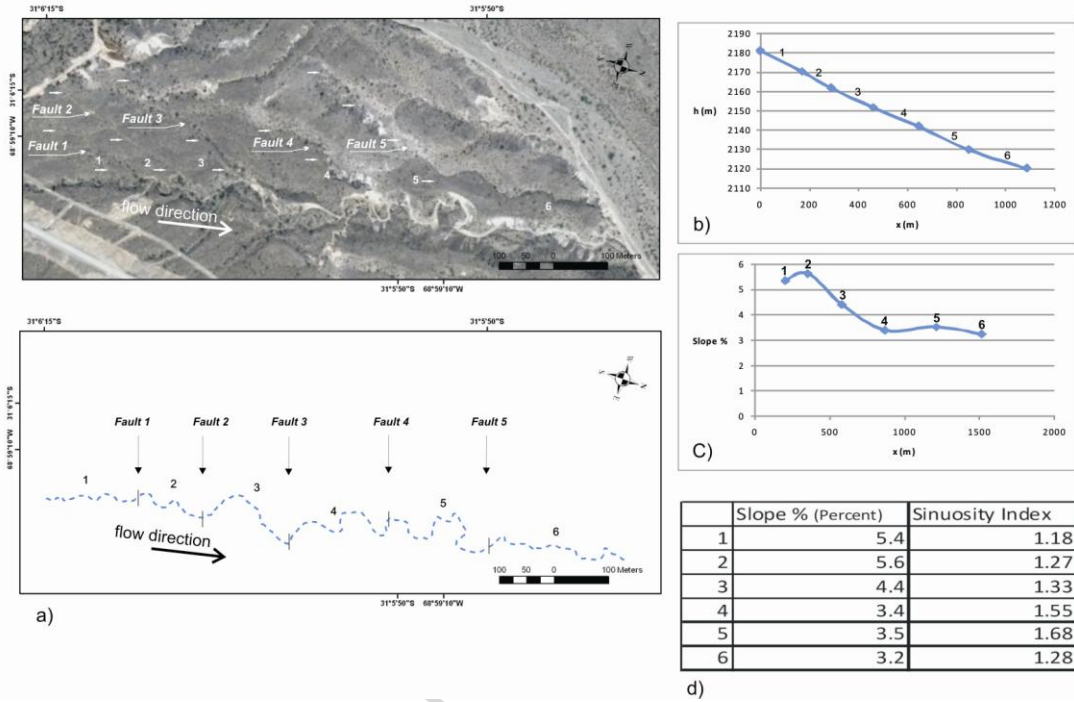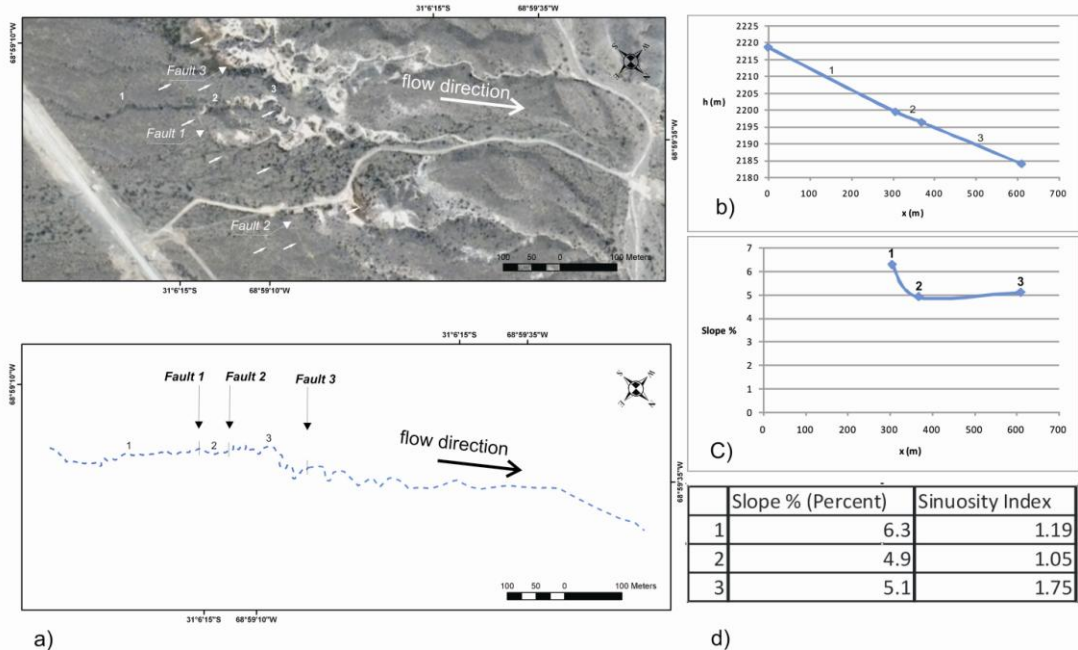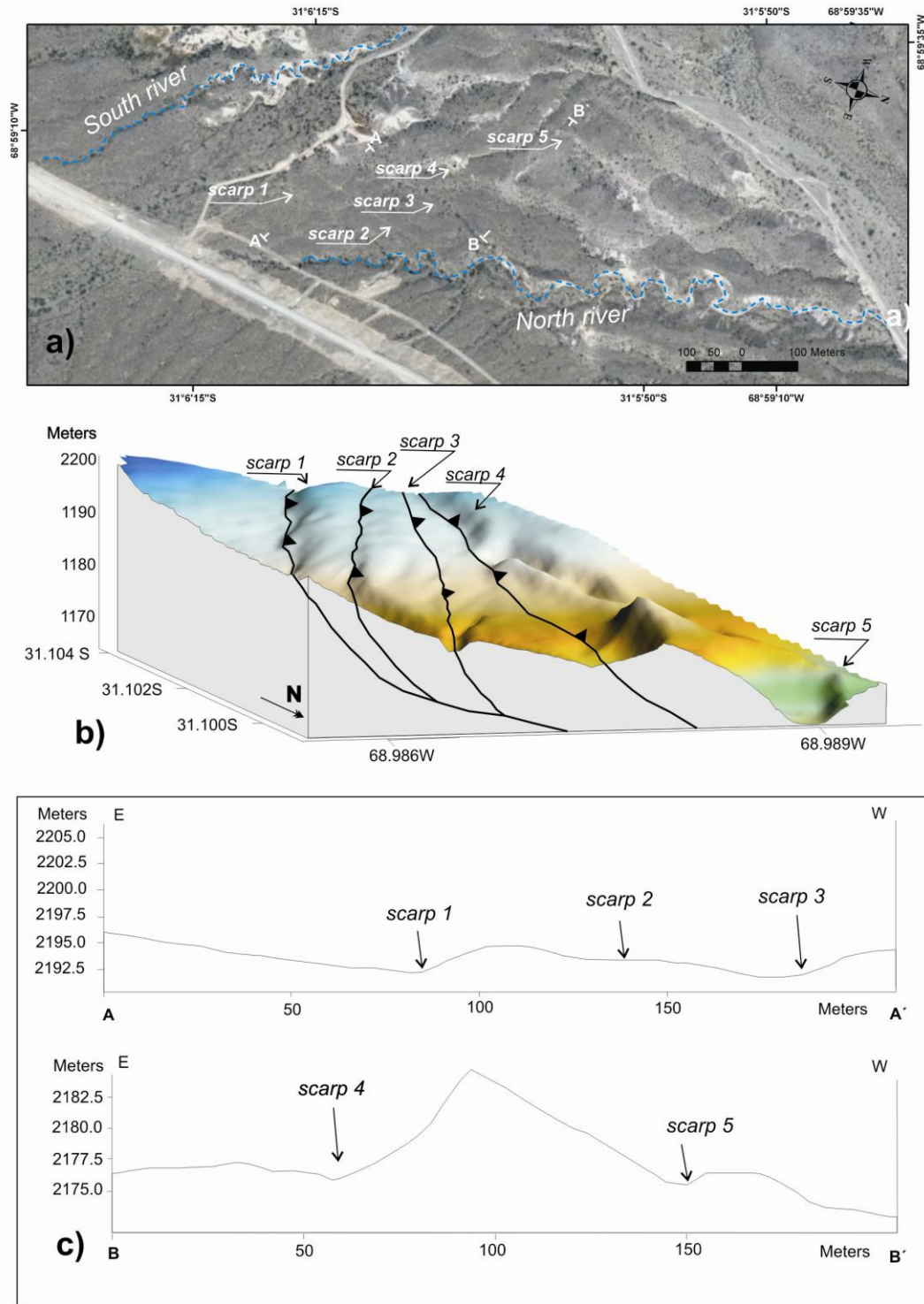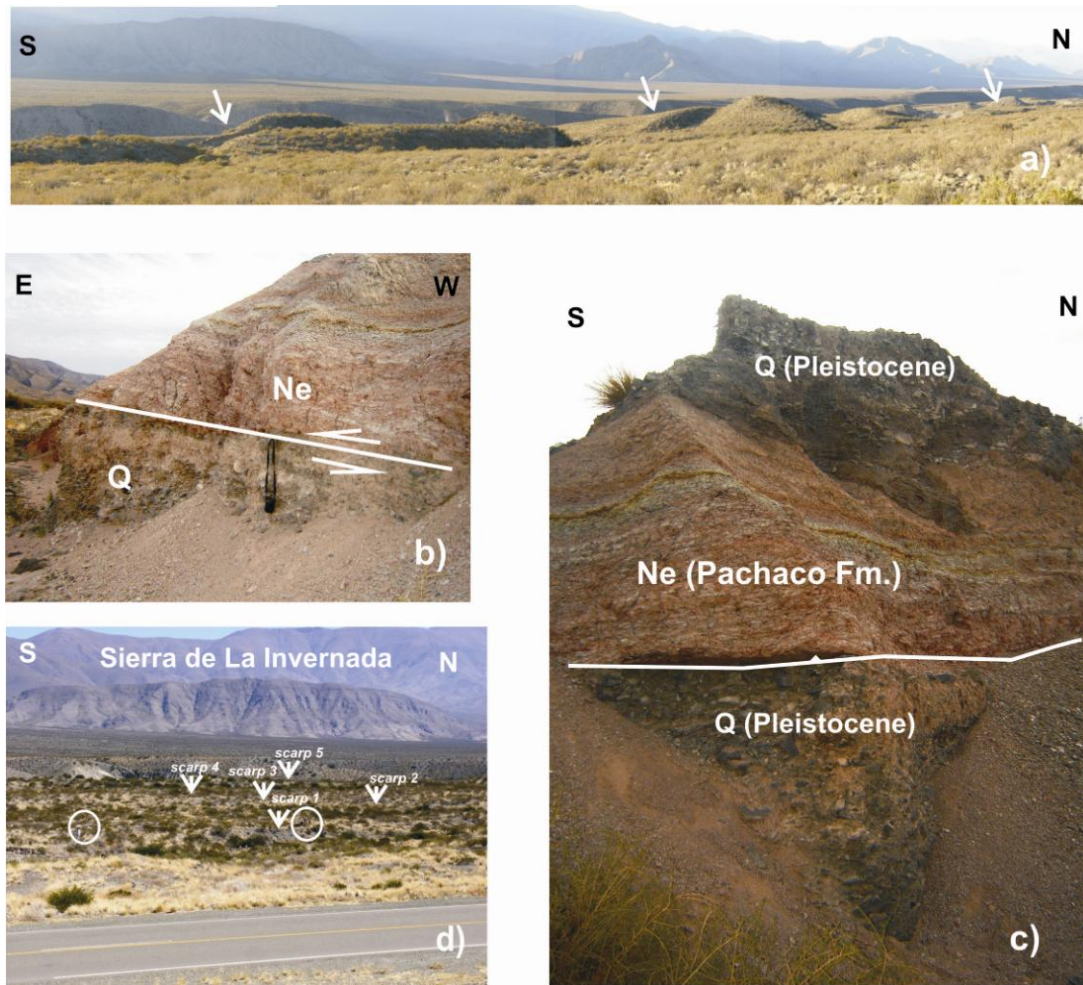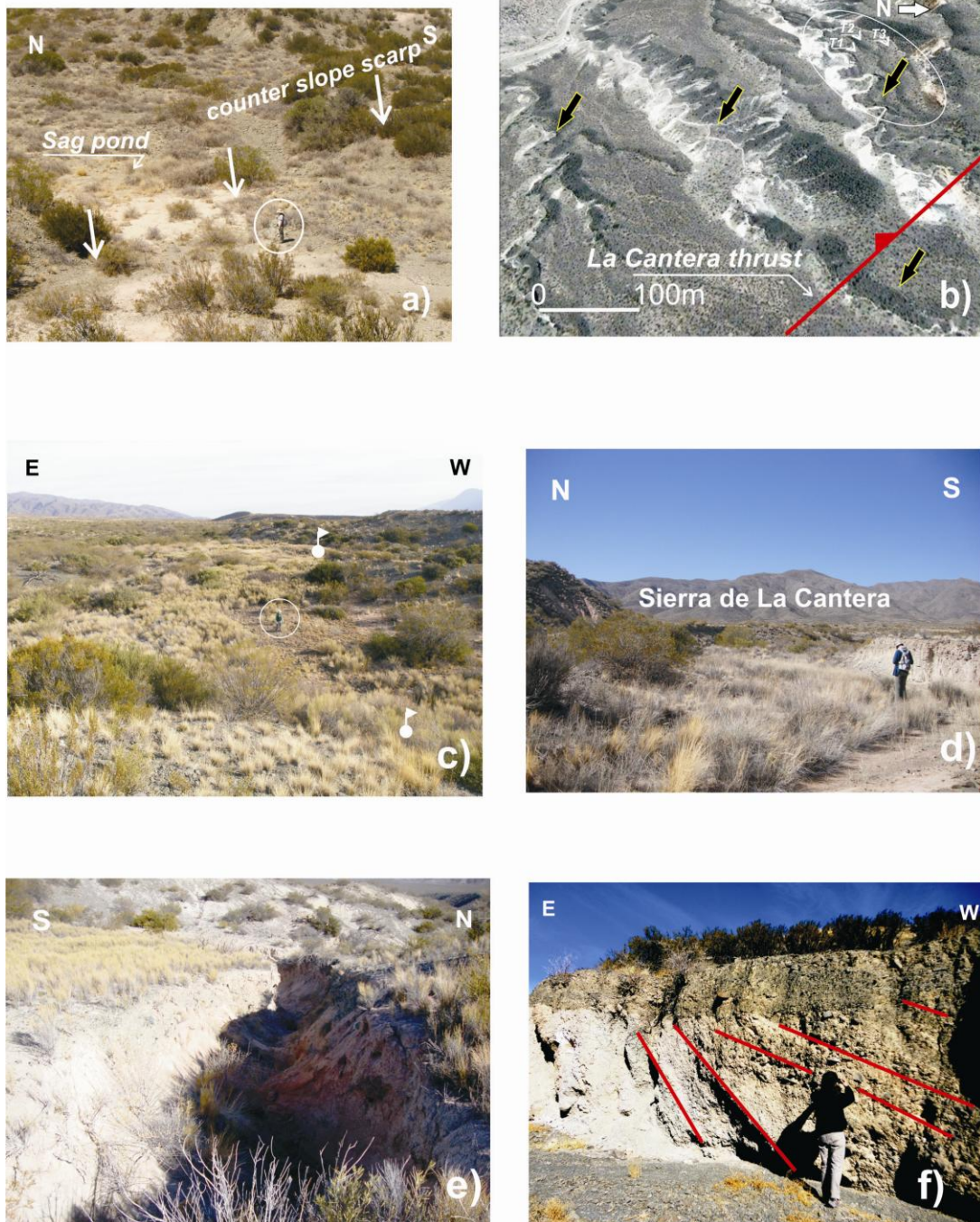
Figure 1

Figure 2

Figure 3

Figure 4

Figure 5

Figure 6

Figure 7